Available online at www.sciencedirect.com
ScienceDirect
Journal of Sound and Vibration 315 (2008) 88–99
JOURNAL OF SOUND AND VIBRATION
www.elsevier.com/locate/jsvi

Sound generated by a jet-excited spherical cavity

A.W. Foley[a], M.S. Howe[a,*], T.A. Brungart[b]

[a]*College of Engineering, Boston University, 110 Cummington Street, Boston MA 02215, USA*
[b]*Applied Research Laboratory, The Pennsylvania State University, State College, PA 16804, USA*

Received 12 September 2007; received in revised form 11 January 2008; accepted 17 January 2008
Handling Editor: P. Joseph
Available online 04 March 2008

Abstract

An analysis is made of the sound generated by the impingement of a high-speed ventilating gas jet on the gas–water interface of a ventilated supercavity. A precise analytical problem is formulated and solved in which the supercavity is modelled by a spherical cavity of equal interior volume and the jet consists of a planar, radially symmetric flow from the centre of the sphere. The gas content of the sphere is assumed to be maintained at a constant mean level by steady exhaust into the water from the 'rear end' of the cavity. It is estimated that the damping of jet-induced oscillations by this outflow is negligible compared with conventional losses produced by acoustic radiation and by viscous and thermal dissipation. The sound radiated into the water is omnidirectional at low frequencies, but with increasing frequency it progressively exhibits the directional characteristics of an acoustic dipole with axis centred on the radial axis of the gas jet.
© 2008 Elsevier Ltd. All rights reserved.

1. Introduction

An underwater vehicle can attain very high speeds if a substantial fraction of it is enclosed within a gaseous envelope or 'ventilated supercavity', which forms a 'cushion' that eliminates conventional skin friction and yields drag reductions of up to 90% [1]. The cavity is initiated at a 'cavitor' at the nose and terminates sufficiently far downstream that it encloses the whole of the aft section of the vehicle except for control surfaces used for guidance (see Ref. [2] for a general discussion and survey). It is maintained in a statistically steady state by the injection of gas just to the rear of the cavitator (Fig. 1). The rate and method of injection are carefully controlled to avoid overpressures and instabilities that can cause the cavity to pulsate [1–4]. Under stable conditions, involving high-speed motion through the water, the gas exhausts from the rear end of the cavity by the quasi-periodic shedding of ring vortices with gaseous cores. At low speeds (i.e. at low Froude numbers, that are not strictly relevant in the present context) the supercavity resembles a hot 'plume' and gas escapes through two trailing, hollow vortex tubes formed by buoyancy-induced plume bifurcation [5].

The cavity is a significant source of aerodynamic sound that can interfere with the proper deployment and operation of the vehicle [6–9]. Turbulence in the aqueous boundary layer approaching the wetted trailing edge of the cavitator from the nose generates sound and hydrodynamic pressure fluctuations as it convects across

*Corresponding author.
E-mail address: mshowe@bu.edu (M.S. Howe).

0022-460X/$ - see front matter © 2008 Elsevier Ltd. All rights reserved.
doi:10.1016/j.jsv.2008.01.039

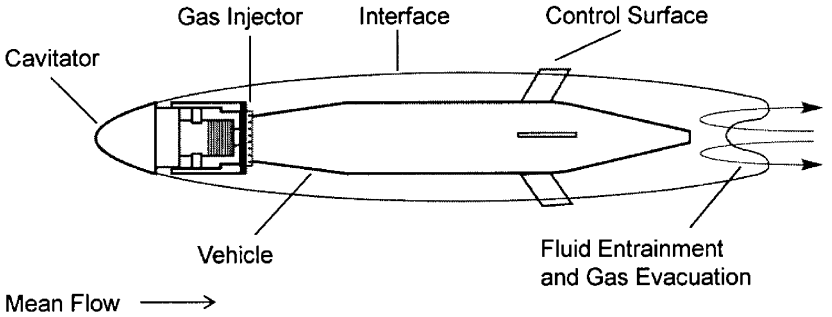

Fig. 1. Schematic experimental supercavity.

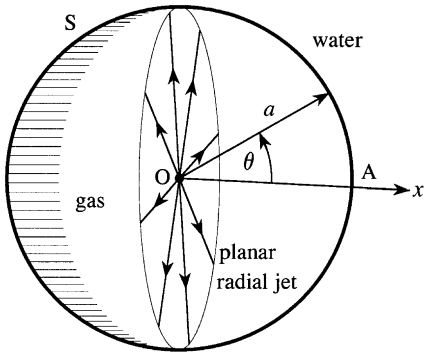

Fig. 2. Configuration of the spherical cavity of radius a and the coordinate system. A thin, axisymmetric planar gas jet flows outwards from the origin in the plane $\theta = \pi/2$. The mean cavity volume is maintained constant by assuming that gas exhausts steadily from the 'rear end' of the cavity by the ejection of quasi-periodic vortex rings (from the vicinity of the point A, for example).

the edge [10–13]. To analyse sources further downstream at non-resonant, higher frequencies that are important in practice, it is reasonable in a first approximation to neglect pressure fluctuations within the cavity, because of the vast difference in mass densities of the gas and water, in which case the gas–water interface can be treated as a 'pressure-release' surface. Then sound generated by turbulence quadrupoles in the flow adjacent to the cavity edge should be relatively unimportant, because the pressure-release interface causes the sound pressure to vary as $\rho_w v^2 M^3$, where the Mach number $M = v/c_w \ll 1$, v being a flow velocity and ρ_w, c_w are, respectively, the mean density and sound speed in water [14]. Bubbles and water droplets in the break-up region of the cavity far downstream are respectively equivalent to monopole and dipole sources [8]; except at extremely high frequencies, their importance is again expected to be greatly reduced by the proximity of the pressure-release cavity.

Observation [12] suggests that the acoustic noise is dominated over a broad range of frequencies by the unsteady impingement of gas on the gas–water interface. Gas from a reservoir flows into the cavity as one or more jets, whose impingement ripples the interface and produces unsteady surface forces and a distributed acoustic surface source of *dipole* type. The acoustic pressure generated by the dipole varies nominally as $\rho_o v_j^2 M$ per unit area of the interface, where ρ_o, v_j denote, respectively, the mean gas density and the velocity of the jet.

In this paper we examine the details of sound generation by the jet. We do this by considering an idealized supercavity of spherical geometry in which the gas enters from the centre in the form of a thin, radially spreading jet (Fig. 2). This canonical model permits general deductions to be made about the sound independently of the difficulties associated with the modelling of a real cavitator and cavity geometries [15–17]. A highly simplified cavity geometry of this kind cannot, of course, represent in detail the acoustics of the real supercavity, but general conclusions relating to source mechanisms and sound waves of characteristic scales that are smaller than the sphere radius should be representative of what happens in practice at high frequencies, whereas predictions at larger length scales (at 'low frequency') should be qualitatively the same.

The mathematical problem is formulated in Section 2 and solved formally by series expansion. Low-frequency cavity resonances excited by the jet are discussed in Section 3; these are likely to dominate the sound radiated to the far field. Higher frequency components of the noise are discussed in Section 4. Specific results and conclusions are drawn by choosing the volume of the cavity to be approximately the same as that of a typical experimental supercavity.

2. The acoustic problem

2.1. Formulation

Consider a spherical cavity of undisturbed radius a in water of mean density ρ_w and sound speed c_w which is at rest at infinity. Let the origin O be at the centre of the cavity (Fig. 2) and introduce spherical polar coordinates (r,θ,ϕ) $(0<\theta<\pi,\ 0<\phi<2\pi)$, where the latitude θ is measured from the positive x direction in the figure. Gas enters the cavity via a thin, axisymmetric planar jet from a source at O, and impinges normally on the cavity interface S along the great circle $\theta=\pi/2$. It is assumed that the mean volume of the cavity and the mean density ρ_o of the gas in the cavity are maintained constant by the steady exhausting of gas into the water from the 'rear end' of the cavity, say the vicinity of the point A in Fig. 2.

Turbulence fluctuations in the jet are assumed to be axisymmetric and to exert an unsteady radial force on the cavity interface equal to $F(t)$ per unit length of the circle of impingement on S. The definition of $F(t)$ is made precise by requiring it to equal the force that would be exerted on the interface by the jet when the interface is assumed to be *rigid*. The forced motion of the interface produces pressure fluctuations $p(r,\theta,t)$ that satisfy

$$\left(\frac{1}{c_o^2}\frac{\partial^2}{\partial t^2}-\nabla^2\right)p=0,\quad r<a,$$
$$\left(\frac{1}{c_w^2}\frac{\partial^2}{\partial t^2}-\nabla^2\right)p=0,\quad r>a, \tag{1}$$

respectively, within the cavity and in the water, where c_o is the mean speed of sound in the gas.

The analytical problem is simplified by introducing the Fourier decomposition $F(t)=\int_{-\infty}^{\infty}F_o(\omega)\mathrm{e}^{-\mathrm{i}\omega t}\,\mathrm{d}\omega$ and considering first the solution for the case where the cavity is excited by a time-harmonic radial force $F_o(\omega)$ per unit length. The solution of the time-dependent problem can subsequently be found by application of the integral operator $\int_{-\infty}^{\infty}(\cdot)\mathrm{e}^{-\mathrm{i}\omega t}\,\mathrm{d}\omega$. Then the time-harmonic pressure $p(r,\theta,\omega)$ satisfies

$$(\nabla^2+k^2)p=0,\quad \text{where}\ \begin{cases}k=k_o=\omega/c_o, & r<a,\\ k=k_w=\omega/c_w, & r>a.\end{cases} \tag{2}$$

The solution in the outer region $r>a$ must exhibit outgoing wave behaviour. The two solutions in $r\lessgtr a$ are related by the conditions that the net pressure and normal displacement are continuous at the interface. Because the force per unit area applied to the interface by the jet is $(F_o/a)\delta(\theta-\pi/2)$, the net pressure is continuous at $r=a$ provided

$$p(a+0,\theta,\omega)=p(a-0,\theta,\omega)+\frac{F_o}{a}\delta\left(\theta-\frac{\pi}{2}\right),\quad 0<\theta<\pi. \tag{3}$$

Similarly, because F_o corresponds to the force exerted on a rigid interface, continuity of normal displacement is satisfied by requiring

$$\frac{1}{\rho_w}\left(\frac{\partial p}{\partial r}\right)_{r=a+0}=\frac{1}{\rho_o}\left(\frac{\partial p}{\partial r}\right)_{r=a-0},\quad 0<\theta<\pi. \tag{4}$$

2.2. Solution in the general case

Within the cavity the time-harmonic solution that remains finite at $r = 0$ has the expansion [8,18]

$$p = \sum_{n=0}^{\infty} A_n j_n(k_o r) P_n(\cos\theta), \quad r < a, \tag{5}$$

where j_n is a spherical Bessel function of the first kind, P_n denotes the Legendre polynomial of order n [19], and the coefficients A_n are to be determined. In the water the pressure is expanded in terms of outgoing radiating waves in the form

$$p = \sum_{n=0}^{\infty} B_n h_n^{(1)}(k_w r) P_n(\cos\theta), \quad r > a, \tag{6}$$

where the B_n are constants and $h_n^{(1)}$ is the spherical Hankel function of the first kind [19].

The coefficients A_n, B_n are calculated from conditions (3) and (4). The first supplies

$$\sum_{n=0}^{\infty} (B_n h_n^{(1)}(k_w a) - A_n j_n(k_o a)) P_n(\cos\theta) = \frac{F_o}{a}\delta\left(\theta - \frac{\pi}{2}\right), \quad 0 < \theta < \pi, \tag{7}$$

which, by means of the orthogonality relation $\int_0^{\pi} P_n(\cos\theta) P_m(\cos\theta)\sin\theta\,\mathrm{d}\theta = 2\delta_{nm}/(2n+1)$ and the formula $P_n(0) = \cos(n\pi/2)\Gamma((n/2)+\frac{1}{2})/\sqrt{\pi}\Gamma((n/2)+1)$ [19], reduces to

$$B_n h_n^{(1)}(k_w a) - A_n j_n(k_o a) = \frac{F_o}{a}\frac{(2n+1)}{2\sqrt{\pi}}\cos\left(\frac{n\pi}{2}\right)\frac{\Gamma((n/2)+\frac{1}{2})}{\Gamma((n/2)+1)}. \tag{8}$$

Condition (4) yields

$$\frac{B_n k_w}{\rho_w} h_n^{(1)'}(k_w a) - \frac{A_n k_o}{\rho_o} j_n'(k_o a) = 0, \tag{9}$$

where the prime denotes differentiation with respect to the argument. Hence

$$\begin{aligned} A_n &= \frac{(2n+1)}{2\sqrt{\pi}}\cos\left(\frac{n\pi}{2}\right)\frac{\Gamma((n/2)+\frac{1}{2})}{\Gamma((n/2)+1)}\frac{F_o}{a j_n(k_o a)(Z_n - 1)}, \\ B_n &= \frac{(2n+1)}{2\sqrt{\pi}}\cos\left(\frac{n\pi}{2}\right)\frac{\Gamma((n/2)+\frac{1}{2})}{\Gamma((n/2)+1)}\frac{F_o Z_n}{a h_n^{(1)}(k_w a)(Z_n - 1)}, \end{aligned} \tag{10}$$

where

$$Z_n = \frac{\rho_w c_w}{\rho_o c_o}\frac{j_n'(k_o a)}{j_n(k_o a)}\frac{h_n^{(1)}(k_w a)}{h_n^{(1)'}(k_w a)}. \tag{11}$$

Now $\cos(n\pi/2) \equiv 0$ when n is odd. Therefore, by replacing n in the above expressions by $2n$, using the result [19]

$$\frac{\Gamma(n+\frac{1}{2})}{\Gamma(n+1)} = \sqrt{\pi}\frac{1\cdot 3\cdot 5\ldots(2n-1)}{2^n n!} \equiv \sqrt{\pi}\frac{(2n)!}{(2^n n!)^2}$$

and substituting into expansions (5) and (6), we deduce the following desired representations of the unsteady pressure within the cavity and radiated into the water:

$$p(r,\theta,\omega) = \frac{F_o}{2a}\sum_{n=0}^{\infty}(-1)^n\frac{(4n+1)(2n)!}{(2^n n!)^2}\frac{P_{2n}(\cos\theta) j_{2n}(k_o r)}{(Z_{2n}-1) j_{2n}(k_o a)}, \quad r < a, \tag{12}$$

$$= \frac{F_o}{2a}\sum_{n=0}^{\infty}(-1)^n\frac{(4n+1)(2n)!}{(2^n n!)^2}\frac{Z_{2n} P_{2n}(\cos\theta) h_{2n}^{(1)}(k_w r)}{(Z_{2n}-1) h_{2n}^{(1)}(k_w a)}, \quad r > a. \tag{13}$$

2.3. Special limiting cases

It is also useful to note the corresponding forms of Eqs. (12) and (13) when (i) the water is regarded as *incompressible* (i.e. when $c_w \to \infty$), and (ii) there is no gas in the cavity ($\rho_o \to 0$).

In case (i) there can be no damping of the sound in the cavity by radiation losses, and we find

$$p(r,\theta,\omega) = \frac{F_o}{2a}\sum_{n=0}^{\infty}(-1)^n \frac{(4n+1)(2n)!}{(2^n n!)^2}\frac{P_{2n}(\cos\theta) j_{2n}(k_o r)}{(Z'_{2n}-1) j_{2n}(k_o a)}, \quad r<a, \tag{14}$$

$$= \frac{F_o}{2a}\sum_{n=0}^{\infty}(-1)^n \frac{(4n+1)(2n)!}{(2^n n!)^2}\frac{Z'_{2n}P_{2n}(\cos\theta)}{(Z'_{2n}-1)}\left(\frac{a}{r}\right)^{2n+1}, \quad r>a, \tag{15}$$

where

$$Z'_n = \frac{-\rho_w k_o a\, j'_n(k_o a)}{\rho_o (n+1) j_n(k_o a)}. \tag{16}$$

In case (ii), where the cavity is treated as a vacuum, $Z_n \to \infty$ and there are no pressure fluctuations within the cavity ($p \equiv 0$ for $r<a$). Then expression (13) reduces to

$$p(r,\theta,\omega) = \frac{F_o}{2a}\sum_{n=0}^{\infty}(-1)^n \frac{(4n+1)(2n)!}{(2^n n!)^2}\frac{P_{2n}(\cos\theta) h^{(1)}_{2n}(k_w r)}{h^{(1)}_{2n}(k_w a)}, \quad r>a. \tag{17}$$

2.4. Suppression of coherent interior modes

Just inside the cavity interface the Bessel function $j_n(k_o r) = \frac{1}{2}(h^{(1)}_n(k_o r) + h^{(2)}_n(k_o r))$ in the expansion (5) of the cavity pressure can be interpreted as representing a component travelling wave $\sim h^{(1)}_n(k_o r)$ *incident* on the interface from within the cavity, and a component $\sim h^{(2)}_n(k_o r)$ *reflected* from the interface. Waves reflected from the interface will subsequently impinge again on the interface, possibly leading to the establishment of coherent resonant oscillations. At high frequencies scattering by small-scale irregularities on the interface will induce incoherence in the interior reflected wave field tending to suppress the growth of coherent resonances. By discarding the *incident* coherent component $h^{(1)}_n(k_o r)$ of the Bessel function we can therefore hope to mimic the effect of random interface scattering.

This is equivalent to repeating the analysis leading to the predictions (12) and (13) with $j_n(k_o r)$ replaced throughout by $h^{(2)}_n(k_o r)$, and yields

$$p(r,\theta,\omega) = \frac{F_o}{2a}\sum_{n=0}^{\infty}(-1)^n \frac{(4n+1)(2n)!}{(2^n n!)^2}\frac{P_{2n}(\cos\theta) h^{(2)}_{2n}(k_o r)}{(\hat{Z}_{2n}-1) h^{(2)}_{2n}(k_o a)}, \quad r<a, \tag{18}$$

$$= \frac{F_o}{2a}\sum_{n=0}^{\infty}(-1)^n \frac{(4n+1)(2n)!}{(2^n n!)^2}\frac{\hat{Z}_{2n}P_{2n}(\cos\theta) h^{(1)}_{2n}(k_w r)}{(\hat{Z}_{2n}-1) h^{(1)}_{2n}(k_w a)}, \quad r>a, \tag{19}$$

where

$$\hat{Z}_n = \frac{\rho_w c_w}{\rho_o c_o}\frac{h^{(2)\prime}_n(k_o a)}{h^{(2)}_n(k_o a)}\frac{h^{(1)}_n(k_w a)}{h^{(1)\prime}_n(k_w a)}. \tag{20}$$

3. Low-frequency resonances

The spectrum of sound radiated to large distances from a cavity tends to be dominated by low frequencies, comparable to the fundamental Minnaert volumetric pulsation frequency [7,20]. This and other resonant oscillations of the cavity are excited by the jet. In this section we examine this excitation. Predictions will be illustrated for the case of an air-filled cavity in water at standard temperature and pressure (STP) when the

cavity has radius $a = 7.0\,\text{cm}$, which corresponds to a cavity volume approximately the same as that of a typical small-scale experimental supercavity.

3.1. Monopole resonances

The monopole is nominally the most efficient source, but it is relevant only at very low frequencies. Volumetric pulsations are then analogous to oscillations of a mass–spring system in which the moving 'mass' is the water displaced radially by the cavity, and the 'spring' stiffness is furnished by the compressibility of the contained gas. The compressibility of the water makes a negligible contribution to the gross motion of the cavity at low frequencies, when the acoustic wavelength is very much larger than the radius a of the cavity. The resonance frequencies can therefore be calculated by ignoring the aqueous compressibility, which is responsible only for relatively weak radiation-damping of the oscillations. This is the only effective damping mechanism except at extremely low frequencies, because viscous and thermal effects are negligible for such large-scale motions (when the acoustic Reynolds number $\gg 1$ [21,22]). However, our model implicitly assumes that the gas content of the cavity is maintained roughly constant by the steady exhausting of the gas into the water, and we shall estimate below the damping arising from this.

According to Eqs. (14) and (15) resonant oscillations of a mode of order $2n$ are determined by the zeros of $(Z'_{2n}(k_o a) - 1)j_{2n}(k_o a) = 0$ when the water is regarded as incompressible, where Z'_{2n} is defined as in Eq. (16). Using the relation $j'_n(z) = j_{n-1}(z) - [(n+1)/z]j_n(z)$, the resonance condition is equivalent to

$$k_o a j_{2n-1}(k_o a) - (2n+1)\left(1 - \frac{\rho_o}{\rho_w}\right) j_{2n}(k_o a) = 0. \tag{21}$$

For the monopole $n = 0$, Eq. (21) reduces to [19]

$$k_o a - \left(1 - \frac{\rho_o}{\rho_w}\right) \tan(k_o a) = 0. \tag{22}$$

When $\rho_o/\rho_w \ll 1$ the smallest positive root of this equation is $k_o a \approx \sqrt{3\rho_o/\rho_w}$, which corresponds to volumetric oscillations at the *Minnaert* radian frequency $\omega = \sqrt{3\rho_o c_o^2/\rho_w a^2}$ [21,22] for which the pressure does not vary with position in the cavity.

For our model cavity of radius $a = 7\,\text{cm}$ the Minnaert frequency $\omega/2\pi \sim 47\,\text{Hz}$. But this mode is actually atypical of monopole resonances, because it corresponds to the special case in which the acoustic wavelength is much larger than the diameter of the cavity. Higher frequency volumetric resonances (determined by the larger roots of Eq. (22)) involve pressure fluctuations within the cavity that oscillate between positive and negative values with distance from the centre. The first ten monopole modes are listed in Table 1: the wavelengths $2\pi/k_o$ of the higher order modes ($N > 1$) are always smaller than the cavity diameter.

The Nth order monopole resonance wavenumber k_o is well approximated at higher frequencies by the formula

$$(k_o a)_N = \frac{(2N-1)\pi}{2}\left\{1 - \frac{4(1-\rho_o/\rho_w)}{(2N-1)^2\pi^2}\right\}, \quad \text{for } N \geqslant 4. \tag{23}$$

3.2. Influence of dissipation

The amplitudes of resonant modes excited by the jet are governed by losses produced by acoustic radiation, possibly by viscous and thermal diffusion at lower frequencies [21,22], and also by hydrodynamic convection

Table 1
Cavity monopole wavenumbers and frequencies at STP (from Eq. (22))

Number N	1	2	3	4	5	6	7	8	9	10
$k_o a$	0.06	4.49	7.73	10.90	14.07	17.22	20.37	23.52	26.67	29.81
Frequency (Hz)	47	3474	5972	8429	10,874	13,312	15,748	18,181	20,614	23,046

of vibrational energy from the cavity by the steady outflow of gas into the water [8]. These mechanisms typically produce small corrections in the values of the resonance frequencies predicted in the absence of dissipation. The first-order effect is that each undamped resonant frequency $\hat{\omega}$, say, is replaced by $\omega \approx \hat{\omega} - \mathrm{i}\varepsilon$, where $\varepsilon = \varepsilon(\hat{\omega}) > 0$ is a small imaginary part that would cause the corresponding unforced resonance to decay in amplitude like $\mathrm{e}^{-\varepsilon t}$. According to Devin [21], when viscous and thermal damping are important their contributions to ε are comparable in magnitude to the radiation damping. We can evaluate the effect of radiation from the solutions (12) and (13), which takes account of the compressibility of the water, i.e. from the solutions of $Z_{2n}(k_o a) - 1 = 0$:

$$\frac{\rho_w c_w}{\rho_o c_o}\frac{j'_{2n}(k_o a)}{j_{2n}(k_o a)}\frac{h^{(1)}_{2n}(k_w a)}{h^{(1)'}_{2n}(k_w a)} = 1, \quad \text{where } k_o = \frac{\omega}{c_o},\ k_w = \frac{\omega}{c_w}. \tag{24}$$

It will be sufficient to consider the damping of the monopole modes ($n = 0$), and in particular the dominant pulsational mode, for which $\hat{\omega}a/c_o \equiv \hat{k}_o a \approx 0.06$ ($N = 1$ in Table 1). By setting $n = 0$ in Eq. (24) we derive the analogue of the undamped frequency equation (22)

$$k_o a - \left(1 - \frac{\rho_o}{\rho_w} + \mathrm{i}k_o a\frac{\rho_o c_o}{\rho_w c_w}\right)\tan(k_o a) = 0 \tag{25}$$

from which the compressible correction to the Minnaert approximation is readily deduced to be:

$$k_o a \approx \hat{k}_o a\left(1 - \mathrm{i}\frac{c_o \hat{k}_o a}{2c_w}\right), \quad \text{where} \quad \hat{k}_o a = \sqrt{\frac{3\rho_o}{\rho_w}}. \tag{26}$$

Therefore, the minimum complex frequency of volumetric resonances is given by

$$\omega = \frac{c_o}{a}\sqrt{\frac{3\rho_o}{\rho_w}} - \mathrm{i}\varepsilon, \quad \varepsilon = \frac{c_o^2(\hat{k}_o a)^2}{2c_w a}, \tag{27}$$

where $\hat{k}_o a \approx 0.06$ (Table 1).

This estimate of the radiation damping coefficient ε should be characteristic of the damping also expected from viscous and thermal losses. However, it is important that it be compared with the hydrodynamic damping produced by the efflux of gas from the 'rear' of the cavity. This is determined by the following argument.

Let $\mathscr{E}$ denote the mean energy density (per unit volume) of the resonance mode within the cavity. The rate at which energy of this mode is removed from the cavity by convection in the gas exhausting into the water is $Q\mathscr{E}$, where Q is the volume velocity of the exhausting gas, which is the same as the volume inflow rate in the jet. Hence, if $V = \frac{4}{3}\pi a^3$ is the cavity volume, the net monopole energy $V\mathscr{E}$ within the cavity decays at a rate determined by

$$\frac{\mathrm{d}\mathscr{E}}{\mathrm{d}t} = -\frac{Q\mathscr{E}}{V}. \tag{28}$$

But $\mathscr{E} \sim |p|^2/\rho_o c_o^2$ and $\mathrm{d}|p|^2/\mathrm{d}t = -2\varepsilon|p|^2$, where ε is the corresponding imaginary part of the resonance frequency associated with hydrodynamic damping, i.e. $\varepsilon = Q/2V$.

Hence, from Eqs. (27) and (28)

$$\frac{\varepsilon_{\text{hydrodynamic}}}{\varepsilon_{\text{radiation}}} \sim \frac{Q/V}{c_o^2(\hat{k}_o a)^2/c_w a}. \tag{29}$$

The typical gas inflow rate $Q \sim 0.01\,\mathrm{m}^3/\mathrm{s}$ for our notional experimental supercavity whose volume is the same as that of a sphere of radius $a = 7\,\mathrm{cm}$, Taking $\hat{k}_o a = 0.06$ and using STP values for the other quantities in Eq. (29), we deduce that

$$\frac{\varepsilon_{\text{hydrodynamic}}}{\varepsilon_{\text{radiation}}} \sim 0.02$$

and therefore that the steady efflux of gas into the water has no significant impact on damping.

Table 2
Quadrupole resonance wavenumbers and frequencies at STP (from Eq. (30))

Number N	1	2	3	4	5	6	7	8	9	10
$k_o a$	3.34	7.29	10.61	13.85	17.04	20.22	23.39	26.55	29.71	32.86
Frequency (Hz)	2585	5636	8205	10,704	13,175	15,632	18,082	20,526	22,967	25,406

This conclusion is doubly true for higher frequency modes which radiate more freely into the water. The implication is that the acoustic properties of the cavity are not significantly influenced by the gaseous exhaust. This is evidently a consequence of pressure continuity across the cavity interface and in the exhaust flow.

3.3. Quadrupole resonances

The case $n = 1$ in Eq. (13) represents a radiation field of quadrupole directivity. The corresponding resonance frequencies when the compressibility of the water is neglected are determined by setting $n = 1$ in Eq. (21), i.e. by the roots of

$$(k_o a)^3 - 9k_o a\left(1 - \frac{\rho_o}{\rho_w}\right) + \left(9 - 4(k_o a)^2 - \frac{3\rho_o}{\rho_w}(3 - (k_o a)^2)\right)\tan(k_o a) = 0. \tag{30}$$

The length scales of these wave modes within the cavity are no larger than the cavity diameter. Indeed it is readily confirmed by expansion of the equation in powers $k_o a$ that there are no solutions satisfying $|k_o a| \ll 1$. Numerical solution of Eq. (30) yields the results in Table 2, where the frequencies tabulated in the third line are for a 7 cm spherical air cavity.

Similar analyses of the resonances can be performed for the higher order modes ($n > 1$ in Eqs. (12) and (13), but it is not necessary to present details here. It is clear that the principal low-frequency resonances occur for $k_o a > 1$, the only exception being the special case of the Minnaert monopole. Experiments on cavitating jets all indicate that the far-field acoustic spectrum peaks in the neighbourhood of a frequency comparable to the Minnaert frequency [7,20] and typically decays like ω^{-2} at higher frequencies. Our results indicate a similar behaviour for the cavity (the corresponding continuum spectrum being formed by the aggregate contributions from the cavity resonances) although the precise details for the spherical cavity and for a practical ventilated supercavity depend on the frequency dependence of the appropriate jet forcing function $F_o(\omega)$.

4. Directivity of the sound

The acoustic far field in the water satisfies $k_w r \gg 1$. In this limit the asymptotic approximation $h_n^{(1)}(z) \approx (-\mathrm{i})^{n+1}\mathrm{e}^{\mathrm{i}z}/z$ permits the reduction of Eq. (13) to the form

$$p(r, \theta, \omega) \approx -\frac{\mathrm{i}F_o \mathrm{e}^{-\mathrm{i}\omega(t - r/c_w)}}{k_w a r} \sum_{n=0}^{\infty} \frac{A_n Z_{2n} P_{2n}(\cos\theta)}{(Z_{2n} - 1)h_{2n}^{(1)}(k_w a)}, \quad k_w r \to \infty, \tag{31}$$

where $A_n = (4n + 1)(2n)!/\{2^{(2n+1)}(n!)^2\}$. Therefore

$$\left|\frac{p(r, \theta, \omega)}{F_o/a}\right|^2 \approx \frac{1}{(k_w r)^2}\left|\sum_{n,m=0}^{\infty} \frac{A_n A_m Z_{2n} Z_{2m} P_{2n}(\cos\theta) P_{2m}(\cos\theta)}{(Z_{2n} - 1)(Z_{2m} - 1)h_{2n}^{(1)}(k_w a)h_{2m}^{(1)}(k_w a)}\right|, \quad k_w r \to \infty. \tag{32}$$

This formula determines the directivity ($\propto |p(r, \theta, \omega)|^2$) of the sound radiated into the water. The directivity is plotted as a function of θ in Fig. 3 (on a polar plot, each curve being normalized with respect to its

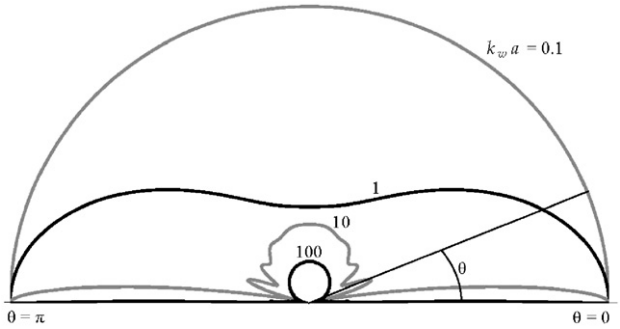

Fig. 3. Directivity of the jet-excited sound for the general case of an air-filled spherical cavity at STP determined by Eq. (32) when $k_w a = 0.1, 1, 10, 100$. Each curve is normalized with respect to its peak value.

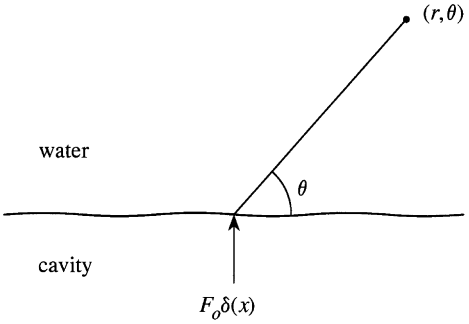

Fig. 4. The problem of sound produced by a two-dimensional jet impinging on a nominally plane interface.

maximum value) for a cavity filled with air at STP when $k_w a = 0.1,\ 1,\ 10,\ 100$. The field shape is spherically symmetric at very low frequencies ($k_w a < 0.1$) characteristic of the Minnaert monopole. As the frequency increases (for $k_w a$ greater than about 10, i.e. for frequencies exceeding 38,600 Hz for a spherical cavity of radius 7 cm) the sound exhibits a progressive tendency to radiate preferentially in the side-line direction with the directivity of the principal side lobe being approximately $\sin^2\theta$, i.e. that of an axisymmetric dipole with axis along the radial direction of the jet.

The dipole radiation is accompanied by narrow beams radiated in the fore and aft directions ($\theta = 0,\ \pi$). The presence of these beams appears to be an artifact of the spherical geometry and would be absent for the more realistic geometries, such as that of the 'cigar'-shaped cavity illustrated in Fig. 1, because the interface is effectively equivalent to a 'pressure release' surface along which sound cannot propagate. This is illustrated by reference to the exact analytical solution for the case of a two-dimensional jet impinging on a plane interface (Fig. 4). For the simplest condition in which the pressure in the cavity (the lower region in Fig. 4) is negligible, the pressure radiated into the water consists entirely of the dipole field

$$p(r,\theta,\omega) \sim \frac{-F_o\sqrt{k_w}\sin\theta e^{i\{k_w r-\pi/4\}}}{\sqrt{2\pi r}}, \quad k_w r \to \infty, \tag{33}$$

where angle θ is defined as in Fig. 4. Therefore, to visualize more clearly the emergence of the dipole we plot the acoustic directivity for the spherical cavity (again, $\propto |p(r,\theta,\omega)|^2$) normalized with respect to its value at $\theta = \pi/2$, clipping the beams in the fore and aft directions, as in Fig. 5.

It is also of interest to compare these predictions with those for two of the special cases discussed in Section 2. In Section 2.4 the effect on sound generation of wave incoherence produced by a randomly irregular cavity interface is modelled by the formal neglect of pressure waves incident on the interface from within the cavity. In this case $|p(r,\theta,\omega)|^2$ in the far-field is given by Eq. (32) with $Z_{2n,2m}$ replaced by $\hat{Z}_{2n,2m}$ defined in

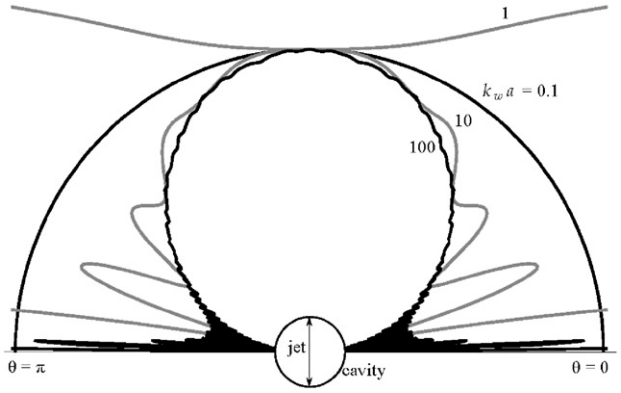

Fig. 5. Directivity of the jet-excited sound for the general case of an air-filled spherical cavity at STP determined by Eq. (32) when $k_w a = 0.1, 1, 10, 100$. Each curve is normalized with respect to its value at $\theta = \pi/2$.

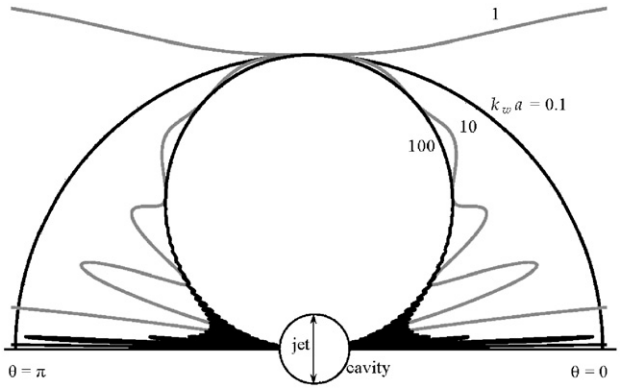

Fig. 6. Directivity of the jet-excited sound when the correction of Eq. (20) is introduced into Eq. (32) to account for incoherent reflection of waves from the interface, for an air-filled spherical cavity at STP when $k_w a = 0.1, 1, 10, 100$. Each curve is normalized with respect to its value at $\theta = \pi/2$.

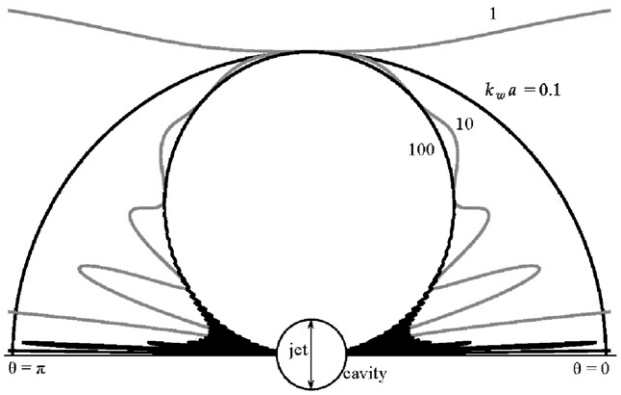

Fig. 7. Directivity of the jet-excited sound in case (ii) of Section 2.3 (a 'vacuous' cavity interior) determined by Eq. (33) for $k_w a = 0.1, 1, 10, 100$. Each curve is normalized with respect to its value at $\theta = \pi/2$.

Eq. (20). The corresponding directivities (in Fig. 6) are seen to be hardly changed from those predicted from Eq. (32) for the full solution, indicating that the directivity of high-frequency sound is essentially unaffected by reflections within the cavity.

Second, in case (ii) of Section 2.3 pressure variations within the cavity are absent (a 'vacuous' cavity interior). It now follows from Eq. (17) that

$$\left|\frac{p(r,\theta,\omega)}{F_o/a}\right|^2 \approx \frac{1}{(k_w r)^2}\left|\sum_{n,m=0}^{\infty}\frac{A_n A_m P_{2n}(\cos\theta)P_{2m}(\cos\theta)}{h_{2n}^{(1)}(k_w a)h_{2m}^{(1)}(k_w a)}\right|, \quad k_w r \to \infty. \tag{34}$$

Again, the typical field shapes plotted in Fig. 7 are effectively identical with the corresponding plots for the full solution.

This agreement occurs because, except at the resonance frequencies, $Z_{2n}/(Z_{2n}-1)\sim\hat{Z}_{2n}/(\hat{Z}_{2n}-1)\sim 1$ when $\rho_w \gg \rho_o$. This conclusion has been confirmed (and the accuracy of the numerical procedure validated) by recalculating the directivities for the fully compressible cavity and for the case of Section 2.4 of incoherent interface scattering in cases where $\rho_o \sim \rho_w$ (but with unchanged values of c_o and c_w). The resulting directivities are consistently found to be *different* from each other, and also different from the results in Figs. 5–7 for an air-filled cavity.

5. Conclusions

The low-frequency sound radiated by the spherical model of a supercavity is dominated by the volumetric monopole modes excited by the jet. The amplitudes of motions near the cavity are controlled predominantly by damping produced by the sound radiation, and to a lesser extent by viscous and thermal losses in the cavity and the steady hydrodynamic flow of gas from the 'rear end' of the cavity. For all frequencies of practical interest, the continuity of pressure across the cavity interface and within the exhaust flow ensures that the hydrodynamic damping is negligible, and therefore that the acoustics of the system are largely unaffected by the gas exhaust flow.

The radiation from the cavity is omnidirectional at low frequencies, comparable to the Minnaert frequency of the dominant monopole. As the frequency increases the radiation directivity develops a principal side-lobe equivalent to that produced by a dipole acoustic source with axis along the radial direction of the gas jet impinging on the interface. Our numerical results for the spherical cavity with a jet impinging at $\theta = \pi/2$ to the nominal direction of the mean water flow indicate that this dipole radiation (of directivity $\sim\sin^2\theta$) is accompanied by narrow beams radiated in the fore and aft directions ($\theta = 0,\ \pi$). These beams are an artifact of the spherical geometry that is likely to be absent in more realistic cavity geometries.

The theoretical results for the spherical cavity indicate that the side-line dipole is well formed when $k_w a > 10$. For the more general cavity this suggests that the dipole becomes prominent at frequencies exceeding about $1.5c_w/\mathscr{R}$ Hz, where $\mathscr{R}$ is the mean radius of curvature of the interface at the point of impact of the jet. At such frequencies, the self-noise generated by the gas jet might be expected to have a negligible influence on control systems situated near the cavitator.

Acknowledgements

The work reported here is sponsored by the Office of Naval Research Code 333, Grant N00014-06-1-0270 under the University/Laboratory Initiative directed by Dr. Kam W. Ng.

References

[1] R. Kuklinski, C. Henoch, J. Castano, Experimental study of ventilated cavities on dynamic test model, Paper presented at Cav2001: Session B3.004, 2001.
[2] J.P. Franc, J.M. Michel, *Fundamentals of Cavitation*, Kluwer Academic Publishers, Dordrecht, 2004.
[3] E. Silberman, C.S. Song, Instability of ventilated cavities, *Journal of Ship Research* 5 (1) (1961) 13–33.
[4] C.S. Song, Pulsation of ventilated cavities, *Journal of Ship Research* 5 (4) (1962) 8–20.
[5] R.S. Scorer, *Natural Aerodynamics*, Pergamon Press, London, 1958.
[6] M.J. Lighthill, On sound generated aerodynamically. Part I: general theory, *Proceedings of the Royal Society of London A* 211 (1952) 564–587.
[7] W.K. Blake, *Mechanics of Flow-induced Sound and Vibration*, Academic Press, New York, 1986.

[8] M.S. Howe, *Acoustics of Fluid–Structure Interactions*, Cambridge University Press, Cambridge, 1998.
[9] M.S. Howe, *Theory of Vortex Sound*, Cambridge University Press, Cambridge, 2003.
[10] M.S. Howe, Surface pressure and sound produced by turbulent pressure-release edge flow, Applied Research Laboratory Technical Memorandum 98-148, Pennsylvania State University, 1998.
[11] S.D. Young, T.A. Brungart, G.C. Lauchle, Effect of a downstream ventilated gas cavity on the spectrum of turbulent boundary layer wall pressure fluctuations, *Proceedings of the IMECE04, 2004 ASME International Mechanical Engineering Congress*, Anaheim, California, November 13–19, 2004.
[12] S.D. Young, T.A. Brungart, G.C. Lauchle, M.S. Howe, Effect of a downstream ventilated gas cavity on the spectrum of turbulent boundary layer wall pressure fluctuations, *Journal of the Acoustical Society of America* 118 (2005) 3506–3512.
[13] M.S. Howe, Sound produced by a vortex interacting with a cavitated wake, *Journal of Fluid Mechanics* 543 (2005) 333–347.
[14] J.E. Ffowcs Williams, Sound production at the edge of a steady flow, *Journal of Fluid Mechanics* 66 (1974) 791–816.
[15] G.V. Logvinovich, *Hydrodynamics of free-boundary flows (1969)*, Israel Program for Scientific Translation, Jerusalem, 1972.
[16] C. Pellone, J.-P. Franc, M. Perrin, Modelling of unsteady 2D cavity flows using the Logvinovich independence principle, *Comptes Rendus Mecanique* 332 (2004) 827–833.
[17] E. Paryshev, Approximate mathematical models in high-speed hydrodynamics, *Journal of Engineering Mathematics* 55 (2006) 41–64.
[18] J.A. Stratton, *Electromagnetic Theory*, McGraw-Hill Book Company, New York, 1941.
[19] M. Abramowitz, I.A. Stegun (Eds.), *Handbook of Mathematical Functions*, Dover Publications, New York, 1972.
[20] C.E. Brennen, *Cavitation and Bubble Dynamics*, Oxford University Press, Oxford, 1995.
[21] C. Devin, Survey of thermal, radiation, and viscous damping of pulsating air bubbles in water, *Journal of the Acoustical Society of America* 31 (1959) 1654–1667.
[22] T.G. Leighton, *The Acoustic Bubble*, Academic Press, New York, 1994.